In-Depth Study on the Effect of Active-Area Scale-Down of Solution-Processed TiO_x

Seungjae Jung, Jaemin Kong, Tae-Wook Kim, Sunghoon Song, Kwanghee Lee, Takhee Lee, Hyunsang Hwang, and Sanghun Jeon

Abstract—The effect of active-area scale-down and improved memory performance of solution-processed TiO_x were investigated using devices with active areas ranging from 50×50 μm^2 to 200×200 nm^2. As the active area decreases, higher operation voltages were required owing to the reduction of unintended extrinsic defects resulting from solution processing. Moreover, faster switching speeds were observed with decreasing active area, which is induced by incremental Joule heating. These scale-down effects provided enhanced reliability characteristics such as highly uniform operation voltages and resistance states and improved pulse endurance by minimizing extrinsic defect-related nonuniformity and introducing additional heating-assisted filamentary switching.

Index Terms—Defect, joule heating, scale-down, solution-processing, titanium oxide, via-hole.

I. INTRODUCTION

IN ORDER to develop reliable resistive random access memory (ReRAM), which is considered as an alternative to flash memory, many oxides such as NiO_x [1], HfO_x [2], ZrO_x [3], ZnO_x [4], TiO_x [5]–[7], $SrZrO_3$ [8], and $Pr_{0.7}Ca_{0.3}MnO_3$ [9] have been studied using conventional vacuum-based processes [1], [2], [5], [9] and solution-based processes [3], [4], [6]–[8]. In particular, solution processing has attracted considerable interest owing to its simplicity, large-area device applications, roll-to-roll processability, and low cost.

Unfortunately, to date, most previous studies on solution-processed ReRAM devices focused on the development of oxide materials, which can be synthesized using sol-gel chemistry [3], [4], [6]–[8]. In general, solution processing requires precursors that are dissolved in organic solvents; hence, it is obvious that the use of a patterning process based on a conventional organic solution-based photolithography technique, including photoresistor coating, mask align, expose, develop, ashing, and cleaning processes, is inevitable to generate an unintended chemical reaction between precursors for solution processing and organic solutions for photolithography. Thus, it is extremely difficult to reduce the active area and to demonstrate nanoscale active-area-dependent studies of solution-processed ReRAM devices. Nevertheless, it is imperative to study the memory properties of solution-processed ReRAM devices with decreasing active area because verifying the memory properties of solution-processed oxide materials in microscale devices hinders our understanding of the intrinsic properties and underlying operation mechanism of the devices, owing to multiple extrinsic defect sources from residues of the precursors natively involved in solution processing, as compared to typical vacuum-processed materials. Therefore, we conducted an in-depth study on the effect of active-area scale-down and the change in memory performance of solution-processed TiO_x-based ReRAM devices in nanoscale regime using scalable via-hole structures (microscale to nanoscale) and simple patterning process using shadow masks, which require no additional organic solution [10].

In our investigations, we used various via-hole structures with an active area ranging from 50×50 μm^2 to 200×200 nm^2 as process vehicles. We investigated the active-area-dependent memory parameters and the change in memory performance of solution-processed TiO_x-based ReRAM devices.

II. EXPERIMENTS

To fabricate our ReRAM devices with varying active areas, a $Pt/Al/TiO_x/W$ stack was introduced in the via-hole structure with a different active area defined by a SiO_2 sidewall. An 80-nm-thick W bottom electrode (with a Ti adhesion layer) was sputtered on a 300-nm-thick SiO_2 layer, and an 80-nm-thick SiO_2 layer was deposited by plasma-enhanced chemical vapor deposition as a sidewall of the via hole. The size of the via hole (i.e., active area of ReRAM) was defined by e-beam lithography and reactive ion etching. The via-hole structure was split into six different parts with dimensions 50×50 μm^2, 10×10 μm^2, 5×5 μm^2, 1×1 μm^2, 500×500 nm^2, and 200×200 nm^2. The TiO_x precursor solution was spin coated to fill the via holes, and then, it was hydrolyzed at room temperature for 1 h in air ($T_{TiO_x} \approx 70$ nm). Subsequently, an Al top electrode and a Pt capping layer were deposited. Finally, postannealing was carried out at a temperature of 150 °C in N_2 ambient. The experimental details of the device fabrication and TiO_x
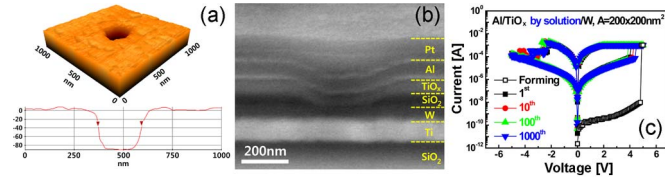
Fig. 1.   (a) AFM image of via-hole structure indicating a depth of 80 nm and bottom width of 200 nm. (b) Cross-sectional SEM image of the fabricated device. (c) Typical bipolar switching curves of the 1st, 10th, 100th, and 1000th cycles for the solution-processed TiO_x-based ReRAM device with an active area of 200×200 nm^2 using double dc voltage sweep mode.

precursor preparation have been provided in our previous paper [6]. The ReRAM device with a 30-nm-thick stoichiometric TiO_x active layer deposited by atomic layer deposition (ALD) was prepared as a counterpart of the solution-processed device with a relatively large number of extrinsic defects.

III. RESULTS AND DISCUSSION

First, we tried to confirm whether the resistive switching properties of TiO_x-based ReRAM devices can be maintained in the nanoscale regime. Fig. 1(a) and (b) show the structural analysis of the fabricated device. In the atomic force microscopy (AFM) image showing the via-hole structure as a process vehicle, the bottom area of 200×200 nm^2 and depth of 80 nm can be clearly seen. The scanning electron microscopy (SEM) image of a tilt view of the fabricated device illustrates the structure of the Pt/Al/TiO_x/sidewall SiO_2/W/Ti/SiO_2 stack. Owing to the inclined sidewall shape prepared under well-modulated dry etching conditions, the via-hole was completely filled with the TiO_x precursor solution, and the active structure of the device was composed of Pt/Al/TiO_x/W/Ti. Fig. 1(c) shows typical bipolar switching curves of the 1st, 10th, 100th, and 1000th cycles for the TiO_x-based ReRAM with an active area of 200×200 nm^2 using the double dc voltage sweep mode. It is important to note that bipolar switching behavior is observed, even with the downscaling of the active area into the nanoscale regime.

In order to investigate the effect of active-area scale-down on resistive switching parameters, the forming, set, and reset voltages of solution-processed TiO_x were monitored as a function of via-hole size [Fig. 2(a)]. As the via-hole size decreased, all the operation voltages increased. However, the increase in the reset voltage was relatively small. This can be explained by the operation mechanism of TiO_x-based ReRAM devices. It is well known that the forming and set processes of TiO_x-based ReRAM occur by the field-induced local alignment of extrinsic defects such as oxygen vacancy [5], [6]. It is evident that the possibility of generating local filaments formed by randomly distributed extrinsic defects increases with increasing active area under a uniformly applied electric field. In particular, as mentioned earlier, solution processing leads to a relatively large number of extrinsic defects, as compared to a typical vacuum-based process; hence, such effects can be strengthened in the case of the forming and set voltages of the solution-processed TiO_x-based ReRAM. This behavior is consistent with that observed in a previous study, which is observed in HfO_x active layers with a relatively high oxygen deficiency [11]. In contrast, since the reset process occurs by the rupture of a preexisting filament owing to the compensation of oxygen vacancies by oxygen atoms and/or Joule heating, the
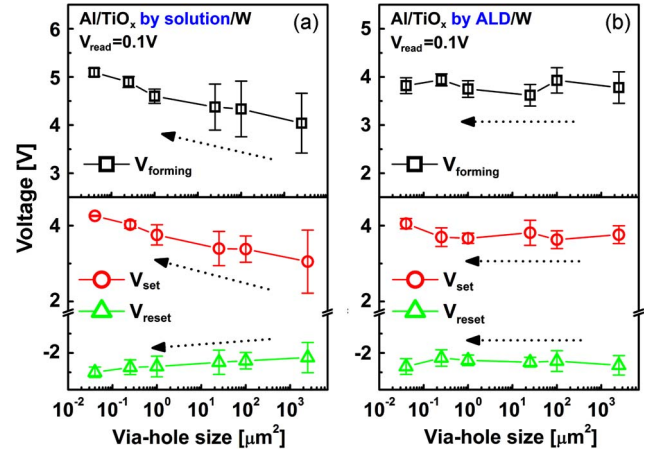
Fig. 2.   Operation voltages as a function of the via-hole size of (a) solution-processed and (b) ALD-processed TiO_x-based ReRAM devices. Each value and its variation correspond to an average and standard deviation, calculated on the basis of data collected from 20 devices.
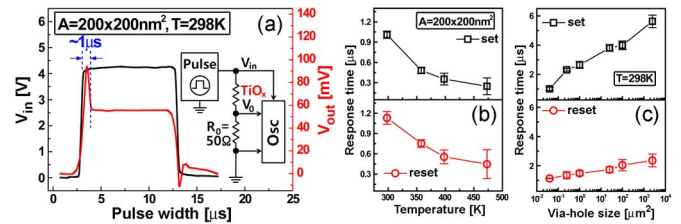
Fig. 3.   (a) Result of response-time delay between input and output pulse signals during the set process and (inset) configuration of measurement setup to monitor delay time. Response-time delay of the set and reset processes as a function of (b) ambient temperature and (c) via-hole size.

dependence of the reset voltage on the reduction of extrinsic defects can be lower than that of the forming and set voltages. To validate our postulation, the result obtained from a relatively stoichiometric TiO_x active layer grown by ALD is shown in Fig. 2(b). X-ray-photoelectron-spectroscopy analysis exhibited that the TiO_x/TiO_2 ratio of the ALD-processed TiO_x active layer was more than two times smaller than that of the solution-processed one (data not shown). As can be expected from the reset voltage behavior of the solution-processed TiO_x-based ReRAM, all the operation voltages of the ALD-processed one changed negligibly as the via-hole size reduced. On the contrary to the solution-processed TiO_x active layer, the initial defect density of the ALD-processed one is significantly low. Therefore, the dependence of active area of the ALD-processed TiO_x active layer on the formation of local filaments caused by extrinsic defects can noticeably lower and thus the changes of all the operation voltages are negligible. Such property is also associated with the relation between initial forming and set voltages. The solution-processed TiO_x active layer with a strong active-area dependence on extrinsic defects showed a large difference between forming and set voltages. On the other hand, a negligible difference between forming and set voltages was observed from the ALD-processed TiO_x active layer, which has a relatively weak dependence of active area on extrinsic defects. Consistent results could also be obtained in a previous report that investigated vacuum-processed NiO active layers with a relatively low oxygen deficiency [12].

Next, the effect of active-area scale-down on switching speed was investigated, as described in Fig. 3. The configuration of the measurement setup capable of monitoring input/output pulse
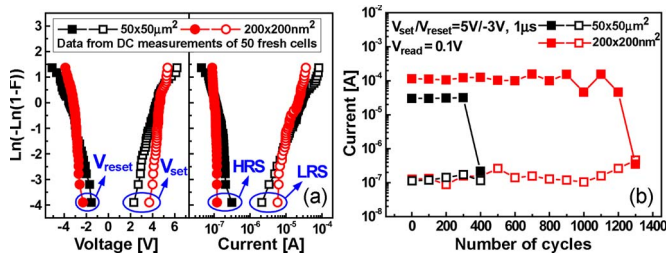
Fig. 4. (a) Area-dependent Weibull plots of V_{SET}, V_{RESET}, HRS, and LRS of the TiO$_x$-based ReRAM device estimated from uniformity tests on 50 fresh devices. (b) Cycling endurance characteristics measured by consecutive voltage pulses ($V_{\mathrm{SET}}/V_{\mathrm{RESET}} = +5$ V, 1 μs$/ - 3$ V, 1 μs, and $V_{\mathrm{read}} = 0.1$ V) of the TiO$_x$-based ReRAM device.

shape is illustrated in the inset of Fig. 3(a), which shows the delay between input and output pulse signals during the set process, thereby indicating a set speed of ~ 1 μs. Using this methodology, we investigated the switching speed of our TiO$_x$ device as a function of temperature [Fig. 3(b)]. As the ambient temperature increases, the delay time decreases during both the set and reset processes, indicating that the migration of extrinsic defects (i.e., oxygen vacancies) and oxygen atoms is enhanced with increasing temperature [9], [11]. Similarly, the flow of an electric current through a conductor generates heat, which is called Joule heating. Since Joule heating is proportional to the square of current density, the increase in the effective temperatures of the active layer can be expected with decreasing via-hole size. Consistent results were observed in the switching-speed-versus-via-hole-size plot [Fig. 3(c)]. The switching speed of both the set and reset processes was improved with decreasing via-hole size. Interestingly, the speed dependence of the reset process was less than that of the set process. Taking into account the switching mechanism of the device on the basis of conducting filamentary, such behavior is considered plausible because the effective active area passing main current flow during the reset process is nearly constant owing to the preexisting filament.

Finally, in order to evaluate the feasibility of the solution-processed TiO$_x$ active layers for high-density memory applications, the uniformity and the repeatability of our ReRAM devices were measured with respect to their active area. Fig. 4(a) shows the area-dependent Weibull plots of the operational voltages and resistance states of the TiO$_x$-based ReRAM, obtained on the basis of the results of uniformity tests on 50 fresh memory devices. Fig. 4(b) shows the cycling pulse endurance characteristics measured by means of consecutive voltage pulses. An improvement in the uniformity of operation voltages and resistance states as well as the switching repeatability, together with a higher on/off ratio under the same set/reset pulse voltage conditions, was achieved in a device with an active area of 200×200 nm^2, as compared to a device with an active area of 50×50 μm^2. These improvements can be explained through the suppression of nonuniform filament formation and thermally assisted set/reset operations, owing to the minimization of the extrinsic defect-related nonuniformity caused by solution processing and enhanced Joule heating by scaling the active area. A similar phenomenon was also observed in variations of the operation voltages [see Fig. 2(a)], when the active area changed.

IV. Conclusion

In this letter, we have investigated the effect of active-area scale-down and the improvement in the memory performance of solution-processed TiO$_x$ using various via-hole structures, with active areas ranging from 50×50 μm^2 to 200×200 nm^2, as process vehicles. Through the evaluation of switching parameters and memory performance depending on via-hole size (i.e., active-area size), the reduction of extrinsic defects and increment of Joule heating have been observed with decreasing via-hole size, which resulted in an increase in operation voltages and improvement of memory performance such as switching speed, pulse endurance, and uniformity of operation voltages and resistance states. We believe that our findings will facilitate the development of solution-processable electronic-device applications by providing more intrinsic resistive switching properties and clear operation mechanisms.

References

[1] M. Lee, S. Han, S. Jeon, B. Park, B. Kang, S. Ahn, K. Kim, C. Lee, C. Kim, I. Yoo, D. Seo, X. Li, J. Park, J. Lee, and Y. Park, "Electrical manipulation of nanofilaments in transition-metal oxides for resistance-based memory," *Nano Lett.*, vol. 9, no. 4, pp. 1476–1481, Mar. 2009.

[2] H. Lee, Y. Chen, P. Chen, T. Wu, F. Chen, C. Wang, P. Tzeng, M. Tsai, and C. Lien, "Low-power and nanosecond switching in robust hafnium oxide resistive memory with a thin Ti cap," *IEEE Electron Device Lett.*, vol. 31, no. 1, pp. 44–46, Jan. 2010.

[3] B. Sun, Y. Liu, L. Liu, N. Xu, Y. Wang, X. Liu, R. Han, and J. Kang, "Highly uniform resistive switching characteristics of TiN/ZrO$_2$/Pt memory devices," *J. Appl. Phys.*, vol. 105, no. 6, pp. 061630-1–061630-4, Mar. 2009.

[4] S. Kim, H. Moon, D. Gupta, S. Yoo, and Y. Choi, "Resistive switching characteristics of sol-gel zinc oxide films for flexible memory applications," *IEEE Trans. Electron Devices*, vol. 56, no. 4, pp. 696–699, Apr. 2009.

[5] D. Kwon, K. Kim, J. Jang, J. Jeon, M. Lee, G. Kim, X. Li, G. Park, B. Lee, S. Han, M. Kim, and C. Hwang, "Atomic structure of conducting nanofilaments in TiO$_2$ resistive switching memory," *Nat. Nanotech.*, vol. 5, no. 2, pp. 148–153, Feb. 2010.

[6] S. Jung, J. Kong, S. Song, K. Lee, T. Lee, H. Hwang, and S. Jeon, "Resistive switching characteristics of solution-processed transparent TiO$_x$ for nonvolatile memory application," *J. Electrochem. Soc.*, vol. 157, no. 11, pp. H1042–H1045, Sep. 2010.

[7] N. Gergel-Hackett, B. Hamadani, B. Dunlap, J. Suehle, C. Richter, C. Hacker, and D. Gundlach, "A flexible solution-processed memristor," *IEEE Electron Device Lett.*, vol. 30, no. 7, pp. 706–708, Jul. 2009.

[8] C. Lin, C. Lin, C. Huanga, C. Lin, and T. Tseng, "Resistive switching properties of sol-gel derived Mo-doped SrZrO$_3$ thin films," *Surf. Coat. Technol.*, vol. 202, no. 4–7, pp. 1319–1322, Dec. 2007.

[9] D. Seong, J. Park, N. Lee, M. Hasan, S. Jung, H. Choi, J. Lee, M. Jo, W. Lee, S. Park, S. Kim, Y. Jang, Y. Lee, M. Sung, D. Kil, Y. Hwang, S. Chung, S. Hong, J. Roh, and H. Hwang, "Effect of oxygen migration and interface engineering on resistance switching behavior of reactive metal/polycrystalline Pr$_{0.7}$Ca$_{0.3}$MnO$_3$ device for nonvolatile memory applications," in *IEDM Tech. Dig.*, 2009, pp. 1–4.

[10] T. Kim, H. Choi, S. Oh, M. Jo, G. Wang, B. Cho, D. Kim, H. Hwang, and T. Lee, "Resistive switching characteristics of polymer non-volatile memory devices in a scalable via-hole structure," *Nanotechnology*, vol. 20, no. 2, pp. 025201, Jan. 2009.

[11] J. Lee, J. Shin, D. Lee, W. Lee, S. Jung, M. Jo, J. Park, K. Biju, S. Kim, S. Park, and H. Hwang, "Diode-less nano-scale ZrO$_x$/HfO$_x$ RRAM device with excellent switching uniformity and reliability for high-density cross-point memory applications," in *IEDM Tech. Dig.*, 2010, pp. 19.5.1–19.5.4.

[12] I. Baek, M. Lee, S. Seo, M. Lee, D. Seo, D. Suh, J. Park, S. Park, H. Kim, I. Yoo, U. Chung, and J. Moon, "Highly scalable non-volatile resistive memory using simple binary oxide driven by asymmetric unipolar voltage pulses," in *IEDM Tech. Dig.*, 2004, pp. 587–590.